

Study on Residual Stress in Viscoelastic Thin Film Using Curvature Measurement Method

Young Tae Im, Seung Tae Choi*, Tae Sang Park

*Department of Mechanical Engineering,
ME3053, KAIST, Science Town, Daejeon 305-701, Korea*

Jae Hyun Kim

*Micro system & Structural Mechanics Group,
KIMM (Korea Institute of Machinery and Materials),
171 Jang-dong, Yusung-ku, Daejeon 305-343, Korea*

Using LSM (laser scanning method), the radius of curvature due to thermal deformation in polyimide film coated on Si substrate is measured. Since the polyimide film shows viscoelastic behavior, i.e., the modulus and deformation of the film vary with time and temperature, we estimate the relaxation modulus and the residual stresses of the polyimide film by measuring the radius of curvature and subsequently by performing viscoelastic analysis. The residual stresses relax by an amount of 10% at 100°C and 20% at 150°C for two hours.

Key Words : Residual Stress, Curvature, Viscoelastic, Elastic-Viscoelastic Correspondence Principle, CTE Mismatch

1. Introduction

In electronic devices or MEMS (micro-electro mechanical system) devices, polyimide films are widely used as dielectric layers because of their excellent thermal stability, good mechanical properties, and low dielectric constant. Thermal deformation due to CTE (coefficient of thermal expansion) mismatch between polyimide and silicon takes place when the polyimide film/Si is cooled down to a room temperature after being coated on Si substrate at high temperature, and this thermal deformation results in thermal stress in the system. The thermal deformation and the induced thermal stress have negative effects on the manufacturing process and sometimes cause the system to fail. Therefore, the measurement of the

thermal deformation is important for evaluating the reliability of film/substrate structures.

Various methods for measuring the residual stresses in film/substrate structures have been developed. For example, X-ray diffraction method, Raman method, and curvature measurement method using optical interferometry or laser scanning can be found in the literature (Nix, 1989; Kampfe, 2000; Laserna, 1996; Courjon et al., 1995; Flinn et al., 1987; Witvrouw et al., 1993). X-ray diffraction method detects the change of lattice spacing due to the occurrence of strains (Kampfe, 2000). Since X-rays usually penetrate multilayers deeply, not only strains but also the information about yielding, cracking, and delamination in the individual layers can be examined. But this method is available only for crystalline materials. Laser Raman spectroscopy deals with the measurement of the radiation scattered from a solid, liquid, or gaseous sample (Laserna, 1996). The characteristic peak in wave spectrum determined by interatomic force is shifted by the change of interatomic distance due to residual stresses. However, to quantify residual stresses,

* Corresponding Author.

E-mail : stchoi@kaist.ac.kr

TEL : +82-42-869-3053; **FAX :** +82-42-869-3095

Department of Mechanical Engineering, ME3053, KAIST, Science Town, Daejeon 305-701, Korea. (Manuscript Received August 1, 2002; Revised November 19, 2003)

this method requires the standard shift of the characteristic peak obtained from the hydrostatic pressure experiments. In curvature measurement method using optical interferometry (Courjon et al., 1995), a simple count of interference fringes permits the determination of curvature. Another effective method of curvature measurement is to use laser-scanning technique, which is based on the principle that a laser beam reflected on a curved surface depends on the orientation of the surface. Flinn et al. (1987) have developed a laser-scanning device that makes use of a rotating mirror to scan the laser beam over a curved surface. In this study, LSM using a translating mirror instead of a rotating mirror is designed to control a laser beam entering the specimen surface.

Analyses of residual stresses in multilayered structures have been performed by many researchers. Stoney (1909) proposed a simple formula known as Stoney's formula for the radius of curvature and the residual stress of a film/substrate system. This formula is applicable when the thickness of film is less than 1/20 of that of substrate. By using the continuity of strain at the interface between substrate and film, Timoshenko (1925) analyzed thin films on a thick substrate. His analysis can take into account the effect of the thickness of films, but cannot be used for multilayered structures having different histories of temperature for each layer. CBA (composite beam analysis) has been developed by Lim et al. (2000) for multilayered structures by means of cut and paste scheme. In CBA, the effect of the thickness of each layer is taken into account and multilayered structures having different histories of temperature for each layer can also be analyzed. These elastic analyses are also useful for materials having viscoelastic properties if the elastic-viscoelastic correspondence principle is valid. In this study, to estimate the relaxation modulus and the stress relaxation in polyimide film, the radius of curvature measured by LSM is analyzed with Stoney's formula and the correspondence principle.

2. Analysis

2.1 Geometric relation for the radius of curvature

LSM makes use of the fact that the direction of laser beam deflected on a specimen surface is dependent on the curvature of the surface. Referring to the geometric relations depicted in Fig. 1, the law of deflection (Hecht, 1998), that the angle between an incident laser and a specimen surface equals the angle between the reflected laser and the surface, yields

$$\Delta d = \Delta x + L(\theta_1 + 2\theta) - L\theta_1 \approx \Delta x + 2L \frac{\Delta x}{R} \quad (1)$$

in which the translation of laser beam in x-direction, Δx , is assumed to be very small enough to have $\Delta x = R\theta$. Then, eq. (1) gives us the radius of curvature in terms of Δx , Δd , and L as follows :

$$R = \frac{2\Delta x}{\Delta d - \Delta x} L \quad (2)$$

2.2 Elastic analysis

Residual stress in thin film bonded on a relatively thick substrate was obtained by Stoney (1909). Thermal deformation due to CTE mis-

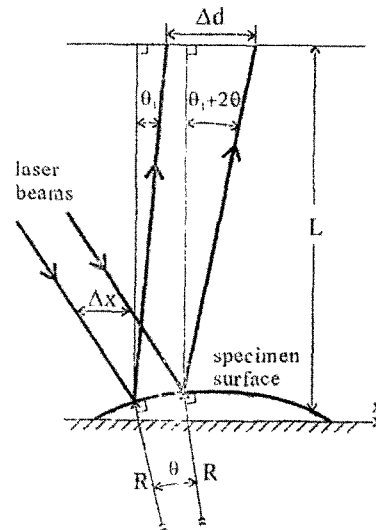


Fig. 1 Geometric relations of laser beams reflected on a specimen surface

match, $\Delta\alpha = \alpha_f - \alpha_s$, where α_f and α_s are CTE of the film and the substrate, respectively, is related to the radius of curvature and the residual stress, σ_f , as follows :

$$\frac{1}{R} = \frac{6\mathcal{M}_f h_f}{\mathcal{M}_s h_s^2} \Delta\alpha \Delta T \quad (3)$$

$$\sigma_f = \mathcal{M}_f \Delta\alpha \Delta T = \frac{\mathcal{M}_f h_s^2}{6R h_f} \quad (4)$$

where ΔT is the temperature excursion. Hereafter, the subscripts s and f refer to the substrate and the film, respectively. $\mathcal{M}_f = E_f / (1 - \nu_f)$ is the biaxial modulus of the film, where E_f and ν_f are Young's modulus and Poisson's ratio of the film, respectively. For the case of cubic crystals, we found that the biaxial modulus of the substrate is $\mathcal{M}_s = (c_{11}^2 + c_{11}c_{12} - 2c_{12}^2) / c_{11}$, where c_{11} and c_{12} are the anisotropic elastic constants of the cubic crystals. It should be noted that the residual stress due to the thermal deformation in the film/substrate structure is the biaxial stress state, even though the substrate has cubic symmetry. Stoney's eq. (3) is applicable when the film thickness, h_f , is less than 1/20 of the substrate thickness, h_s , and the film and the substrate are linear elastic (Nix, 1989). In case of thick film ($h_f > h_s/20$), CBA can take into account the effect of the film thickness, in which the radius of curvature and the residual stress are written as follows (Lim et al., 2000) :

$$\frac{1}{R} = \frac{6\mathcal{M}_f h_f \Delta\alpha \Delta T}{\mathcal{M}_s h_s^2} \left(\frac{h_s + h_f}{h_s + \mathcal{M}_f h_f / \mathcal{M}_s} \right) \quad (5)$$

$$\sigma_f = \mathcal{M}_f \Delta\alpha \Delta T \frac{\mathcal{M}_s h_s}{\mathcal{M}_s h_s + \mathcal{M}_f h_f} = \frac{\mathcal{M}_f \mathcal{M}_s h_s (h_s + h_f)}{R (2\mathcal{M}_s h_s + \mathcal{M}_f h_f)} \quad (6)$$

2.3 Viscoelastic analysis

Polymeric materials like polyimide usually have viscoelastic behavior at elevated temperature (Findley et al., 1976), which may be described by viscoelastic constitutive relation,

$$\sigma(t; T) = \int_0^t \mathcal{M}(t - \tau; T) \frac{d\varepsilon(\tau)}{d\tau} d\tau \quad (7)$$

for biaxial stress state, where $\sigma(t)$ and $\varepsilon(t)$ are the biaxial stress and strain, respectively. While the stresses are being relaxed, the temperature field is assumed to be constant and uniform. The

biaxial relaxation modulus, $\mathcal{M}(t - \tau; T)$ in eq. (7) is a function of elapsed time $t - \tau$ and temperature T . The basic postulate of thermorheologically simple material (Christensen, 1982), which the polyimide film is assumed to be, is

$$\mathcal{M}_f(t; T) = \mathcal{M}_f[t\chi(T)] \quad (8)$$

in which the shift function, $\chi(T)$, should be determined experimentally. The determination of $\chi(T)$ at finite number of different T will be explained in section 4.2. With the elastic-viscoelastic correspondence principle (Christensen, 1982), the radius of curvature and the residual stress in eqs. (3) and (4) for elastic film/substrate structures can be converted to Laplace-transformed viscoelastic solutions, of which the inverse transform gives us

$$\frac{1}{R(t; T)} = \frac{6\mathcal{M}_f[t\chi(T)] h_f}{\mathcal{M}_s h_s^2} \Delta\alpha \Delta T \quad (9)$$

$$\sigma_f(t; T) = \mathcal{M}_f[t\chi(T)] \Delta\alpha \Delta T = \frac{\mathcal{M}_s h_s^2}{6h_f} \frac{1}{R(t; T)} \quad (10)$$

for a given ΔT (ΔT is the temperature difference).

We used eqs. (9) and (10) in analyzing the effect of viscoelasticity since the specimens we used, to be explained next, have films thin enough. However, for future study, we present the result for R and σ_f in thick specimen as follows : The elastic-viscoelastic correspondence principle is applied to CBA model for thick film/substrate structure, consequently for the case of viscoelasticity the radius of curvature and the residual stress in eqs. (5) and (6) are modified respectively as

$$\frac{1}{R(t; T)} = \frac{6h_f(h_s + h_f) \Delta\alpha \Delta T}{h_s^2} \mathcal{G}^{-1} \left\{ \frac{\bar{\mathcal{M}}(s)}{\mathcal{M}_s h_s + s \bar{\mathcal{M}}_f(s) h_f} \right\} \quad (11)$$

$$\sigma_f(t; T) = h_s \Delta\alpha \Delta T \mathcal{G}^{-1} \left\{ \frac{\bar{\mathcal{M}}_f(s) \mathcal{M}_s}{\mathcal{M}_s h_s + s \bar{\mathcal{M}}_f(s) h_f} \right\} = \frac{6h_f(h_s + h_f)^2 \Delta\alpha \Delta T}{h_s^2} \mathcal{G}^{-1} \left\{ \frac{s(\bar{\mathcal{M}}_f(s))^2 \mathcal{M}_s}{(\mathcal{M}_s h_s + s \bar{\mathcal{M}}_f(s) h_f) (2\mathcal{M}_s h_s + s \bar{\mathcal{M}}_f(s) h_f)} \right\} \quad (12)$$

where a bar over a modulus designates its Laplace transformed quantity, and s is the transform variable.

3. Experiment

3.1 Specimen preparation

Thermoplastic polyimide is spin-coated on p-type (100) silicon wafer with $400\ \mu\text{m}$ thickness and 3-inch diameter. Polyimide is a common dielectric, of which glass transition temperature, $T_g=400^\circ\text{C}$, is high enough to stand the process of metal depositions. Polished silicon wafer on which polyimide solution has been put is rotated with 1000 rpm for 10 seconds and 1800 rpm for 30 seconds. The solvent of the coated polyimide solution is removed under $250^\circ\text{C}/1\ \text{hr}/\text{vacuum}$ condition. Then we get $15\ \mu\text{m}$ -thick polyimide film on silicon substrate, which is assumed to be in stress-free state at $T_m=250^\circ\text{C}$.

3.2 Curvature measurement using LSM

LSM using translating mirror is adopted to measure the radius of curvature as shown in Fig. 2. Since LSM is limited to specimens having a mirror surface, laser beams scan the silicon surface of the polyimide/Si specimen, instead of the polyimide surface. The translational displacement in x-direction instead of the angle of the mirror is controlled by the translation stage. With the linear encoder, the translational displacement, Δx , can be measured within $0.5\ \mu\text{m}$ resolution. The laser beam reflected on the specimen surface enters PSD (position sensitive photodetector), which can detect the translation, Δd , in x-direction

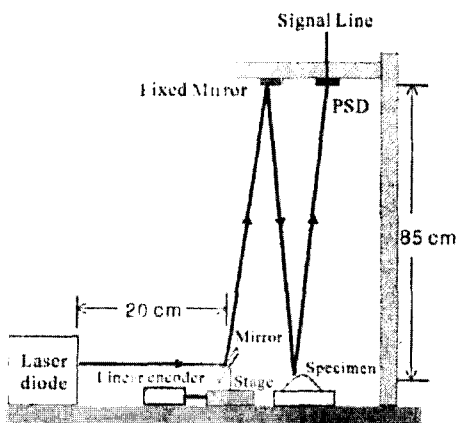


Fig. 2 Schematic diagram of experimental apparatus

tion of the reflected laser beam. By using eq. (2), the radius of curvature of the specimen is measured. The resolution of PSD is $0.15\ \mu\text{m}$ and the distance, Δd , between PSD and the specimen is $0.85\ \text{m}$. Since $\Delta d - \Delta x$ cannot be less than the resolution of PSD, the maximum radius of curvature measurable with the apparatus shown in Fig. 2 is $2.27\ \text{km}$ for $\Delta x=200\ \mu\text{m}$, which corresponds to $1.28\ \mu\text{m}$ deflection at the center of the specimen with 3-inch diameter. The error in measuring the radius of curvature is expected to be less than 5%.

3.3 Viscoelastic property measurement

Relaxation moduli of the polyimide are functions of time and temperature as described in section 2. The standard linear solid model (Ward et al., 1993) is introduced for the polyimide film to get

$$E_f(t; T) = E_\infty + E_0 \exp\left[-\frac{t}{\tau} \chi(T)\right] \quad (13)$$

with $\nu_f=0.4$ (Lim et al., 2000).

While manufacturing the multi-layered structures, another film is deposited onto the polyimide film/substrate, therefore, the polyimide film is exposed to a higher temperature, say, $T=250^\circ\text{C}$, at which the residual stress in the film relaxes. One of the purposes of this study is, to measure the amount of stress relaxation at a higher temperature. There is no stress relaxation at $T=T_r$ (room temperature), as will be seen in Fig. 4(a), while the curvature measurement can only be performed at $T=T_r$. We, therefore, employed the following procedures to obtain the curvature at a higher temperature by measuring it at $T=T_r$.

The specimen, coated at $T_m=250^\circ\text{C}$ is assumed to be stress-free (point A in Fig. 3(a)) at T_m and it is cooled to $T=T_r=20^\circ\text{C}$, at which the curvature is measured (point J_0 in Fig. 3(a)). Then, heating it to $T=T_h=150^\circ\text{C}$ (point H_0 in Fig. 3(a)), it is kept at T_h until $t=t_1$ (point H_1), making the stress relaxation develops. Cooling it to T_r (point J_1), we measure the curvature at T_r . By repeating the above procedures, we can measure the curvatures (equivalently, σ_f) at

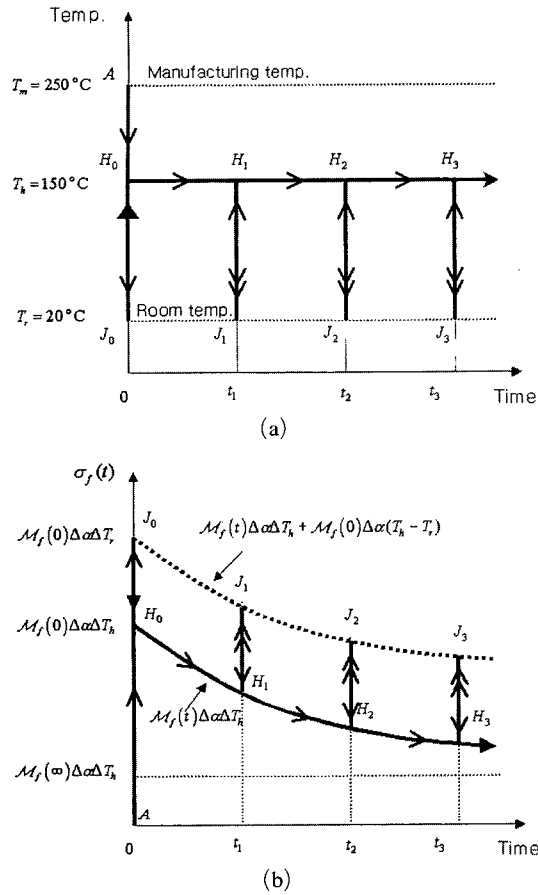


Fig. 3 (a) Temperature history of the specimen and (b) Results of the measurements of residual stresses at $t=0, t_1, t_2, t_3$ at $T_r=20^\circ\text{C}$ (dotted lines J_0, J_1, J_2, J_3) and assumed residual stresses at $t=0, t_1, t_2, t_3$ at $T_h=150^\circ\text{C}$ (solid lines H_0, H_1, H_2, H_3). The difference, $J_0 - H_0 = J_1 - H_1 = J_2 - H_2 = J_3 - H_3$ represents that of the elastic residual stress. ($\Delta T_r = T_m - T_r$ and $\Delta T_h = T_m - T_h$)

points J_0, J_1, J_2, J_3 as shown in Fig. 3(b), plotted in dotted lines.

The residual stresses at $T = T_h$ (the curve H_0, H_1, H_2, H_3), however, are different from those measured (the curve J_0, J_1, J_2, J_3), the difference being the elastic part of the residual stress, i.e. $\mathcal{M}_f(0)\Delta\alpha(T_h - T_r)$. This elastic contribution to the residual stress should be independent of the time elapsed, hence $J_0 - H_0 = J_1 - H_1 = J_2 - H_2 = J_3 - H_3$. The required time to measure the curvature at T_r is about 5 minutes, which does not

affect the amount of stress relaxation since at T_r there hardly occurs stress relaxation. Also, the time required from point J_1 to H_1 is within 10 secs, therefore, its effect can be neglected.

4. Results and Discussion

Experiment has been performed for 3 polyimide/Si specimens prepared according to the procedure described in section 3. Laser scanning is carried out on the diameter of Si wafer running to $\langle 011 \rangle$ direction for all specimens. Since the specimens are in the biaxial stress state, all the radii of curvature must be independent of measuring directions on the specimen surfaces. Since the thickness ratio of the polyimide film and the Si substrate used in our experiment is $h_f/h_s = 3/80$, Stoney's formulae, eqs. (3) and (4), and the viscoelastic solutions, eqs. (9) and (10), obtained by applying the correspondence principle to Stoney's formulae are used instead of the results of CBA, eqs. (5), (6), (11), and (12). The material properties of Si are $c_{11} = 165.7$ GPa, $c_{12} = 63.9$ GPa, $c_{44} = 79.6$ GPa, and $\alpha_s = 2.6$ ppm/ $^\circ\text{C}$ (Lim et al., 2000; Suwito et al., 1999). The CTE of the polyimide film is $\alpha_f = 40$ ppm/ $^\circ\text{C}$ (Lim et al., 2000), which is assumed to be constant below the glass transition temperature. Relaxation modulus of the polyimide film are measured, as described below.

4.1 Thermal deformation at room temperature and $t=0$

Single crystalline silicon wafers usually have not only surface roughness but also surface curvature after polishing. Before coating a polyimide film on Si substrate, the radius of curvature of polished silicon surface is measured in order to investigate the pure effect of the thermal deformation. The relation below is used:

$$\frac{1}{R_t} = \frac{1}{R_a} - \frac{1}{R_b} \quad (14)$$

in which R_b and R_a are the measured radii of curvature before and after coating, respectively, and R_t is the radius of curvature purely due to thermal deformation (Table 1). Young's modulus,

Table 1 Measured values of radius of curvature, Young's modulus, and residual stress at room temperature and $t=0$

Specimen no.	#1	#2	#3	Avg.	
R_0 (m)	85.0	56.7	34.0	—	
R_t (m)	20.6	19.5	17.4	19.2	
Stoney	E_f (GPa)	1.09	1.15	1.29	1.18
	σ_f (GPa)	15.6	16.5	18.5	16.9
CBA	E_f (GPa)	1.05	1.11	1.24	1.13
	σ_f (GPa)	14.9	15.8	17.8	16.2

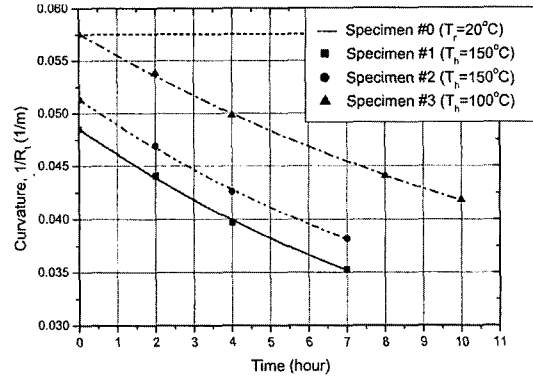
$E_f(0; T)$, (assumed to be temperature independent as in eq. (13)) and the residual stress, $\sigma_f(0; T)$, of the polyimide film at room temperature are calculated by eqs. (9) and (10) with $E_f(0; T) = \mathcal{M}_f(0; T) (1 - \nu_f)$, $\Delta T = 230^\circ\text{C}$, and $\nu_f = 0.4$. The averaged Young's modulus and residual stress are $E_f(0; T) = 1.18$ GPa and $\sigma_f(0; T) = 16.9$ MPa, respectively, as given in Table 1. It is found that the stress relaxation does not take place at $T = T_r = 20^\circ\text{C}$, i.e., R_t is constant at T_r . Since the stress relaxation hardly occurs at room temperature, we set $\chi(T_r = 20^\circ\text{C}) = 0$, which gives us that $E_f(t; T_r) = 1.18$ GPa and $\sigma_f(t; T_r) = 16.9$ MPa are constant, regardless of the elapsed time.

4.2 Curvature, relaxation modulus, and stress relaxation at elevated temperature and $t \neq 0$

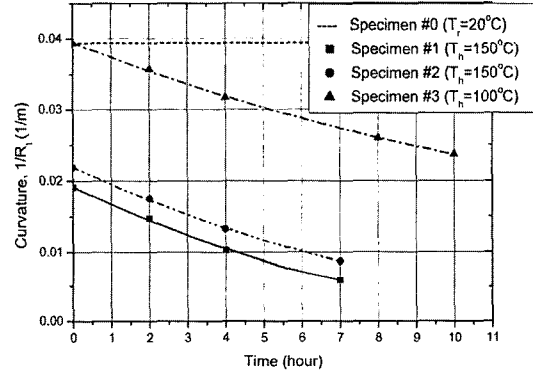
The curvatures of two specimens (#1 and #2) maintained at 150°C and one (#3) at 100°C , respectively, are measured and plotted against time in Fig. 4(a). The curvatures $1/R_t$ in Fig. 4(a) are the results measured at J_0, J_1, J_2, J_3 with the temperature history $J_0-H_0-H_1-J_1-H_1-H_2-J_2-H_2-H_3-J_3$, shown in Fig. 3(a). On the other hand, the curvatures $1/R_t$ in Fig. 4(b) are the assumed values, computed in the following way :

$$\begin{aligned} & \frac{1}{R_t} (\text{Assumed at } T_h) \\ &= \frac{1}{R_t} (\text{measured at } T_r) - \frac{1}{R_t(\text{at } T=T_r, t=0)} \frac{T_h - T_r}{T_m - T_r} \end{aligned} \quad (15)$$

As explained in section 3.3, the second term on the right hand side of eq. (15) (including the



(a)



(b)

Fig. 4 (a) Measured values of curvature at room temp. and (b) assumed values of curvature by eq. (15)

sign) represents the difference of the residual stress at $T = T_h$ and $T = T_r$, i.e., the difference of the elastic residual stresses, which is linear in $(T_h - T_r)$, and independent of time elapsed. In other words, substitute the second term on the right hand side of eq. (15) for R in eq. (4), it can be shown that the calculated value results in $\mathcal{M}_f(0) \Delta \alpha (T_h - T_r)$, the difference of the residual stresses at T_h and T_r .

The curvature of the specimen #3 is larger than those of the specimens #1 and #2, which means that the residual stress in the specimen #3 is larger than those in the specimens #1 and #2. As time elapses, the curvatures exponentially decrease, which corresponds to the stress relaxation. With the graph of the measured curvatures vs. time (Fig. 4) and the standard linear solid model, eq. (13), the relaxation modulus of the polyimide

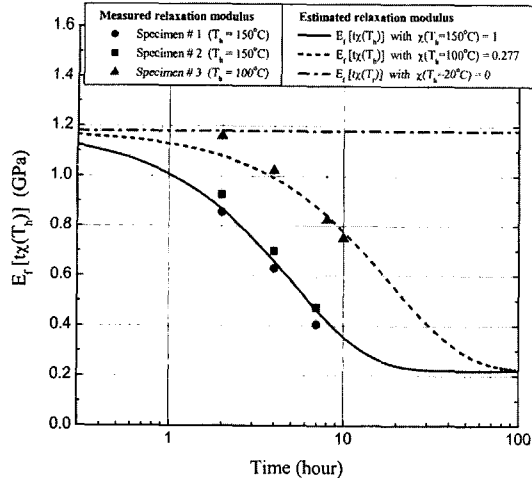


Fig. 5 Relaxation modulus of the polyimide film is estimated by the measured values to be $E_f(t; T) = 0.2207 + 0.9593 \exp[-t\chi(T)/5.08 \text{ hr}]$ together with the values of the shift function, $\chi(T) = 0, 0.227$, and 1 , at $T = 20^\circ\text{C}$, 100°C , and 150°C , respectively

film is curve-fitted to be

$$E_f(t; T) = 0.2207 + 0.9593 \exp\left[-\frac{t\chi(T)}{5.08}\right] (\text{GPa}) \quad (16)$$

together with the shift function. The shift function $\log \chi(T)$ is a linear function of temperature (Hwang et al., 2003), the values of the shift function are $\chi(T) = 0, 0.227$, and 1 , at $T = 20^\circ\text{C}$, 100°C , and 150°C , respectively (Fig. 5). In fitting the curve, we choose $\chi(T) = 1$ at $T = 150^\circ\text{C}$. The time constant of the relaxation modulus, eq. (16), is $\tau = 5.08$ hour, which is large enough to ignore the 5-minute interruptions spent to measure the radius of curvature. At $t = 0$, $E_f(0; T) = 1.18$ GPa regardless of temperature. As time goes to infinity, $E_f(t; T)$ approaches $E_\infty = 0.2207$ GPa. In Fig. 5, if the relaxation function for $T_h = 100^\circ\text{C}$ is shifted to the left by an amount of $|\log \chi(100^\circ\text{C})| = 0.652$, the relaxation function for $T_h = 100^\circ\text{C}$ coincides with that for $T_h = 150^\circ\text{C}$. The residual stresses are also calculated by the obtained relaxation modulus, eq. (16), and eq. (10), $\sigma_f(t; T) = M_f[t\chi(T)]\Delta\alpha\Delta T$, where the biaxial modulus is related to the relaxation modulus by $M_f(t; T) = E_f(t; T)/(1 - \nu_f)$

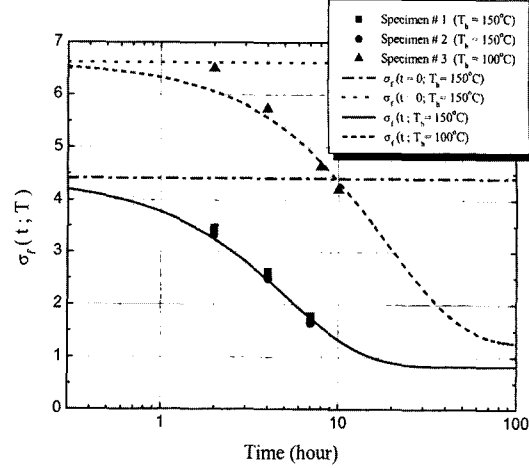


Fig. 6 Residual stresses due to CTE mismatch at $T_h = 100^\circ\text{C}$ and 150°C

(Fig. 6). The dotted and broken horizontal lines in Fig. 6 denote the residual stresses at $T_h = 100^\circ\text{C}$ and $T_h = 150^\circ\text{C}$, respectively (at $t = 0$), which are simply $M_f(0)\Delta\alpha\Delta T_h$. Since the temperature jump, $\Delta T_h = T_m - T_h$, for $T_h = 100^\circ\text{C}$ is larger than that for $T_h = 150^\circ\text{C}$, the residual stress at 100°C is larger than that at 150°C , and the stress relaxation at 150°C takes place faster than at 100°C . It relaxes by an amount of 10% at 100°C and 20% at 150°C for two hours after manufacturing. As time goes to infinity, the residual stress approaches $M_f(\infty)\Delta\alpha\Delta T_h$. Were it not for the viscoelastic effect of the polyimide film, the residual stresses would be overestimated by the amount of $[M_f(0) - M_f(\infty)]\Delta\alpha\Delta T$, which corresponds to about 80% of the residual stresses at $t = 0$.

5. Conclusions

Experimental apparatus using LSM is developed for measuring the radius of curvature due to the thermal deformation in polyimide film coated on Si substrate. The system is capable of detecting the radius of curvature up to about 2.27 km. This LSM is limited to specimens having a mirror surface. After manufacturing the polyimide/Si specimens at 250°C , the specimens are maintained at elevated temperature, $T_h = 150^\circ\text{C}$ (or 100°C). Relaxation modulus and stress relaxation in the

polyimide film are estimated by measuring the values of the radius of curvature at an interval of about 2 hours, and then, by performing the viscoelastic analysis, which is based on the elastic-viscoelastic correspondence principle. At room temperature, the stress relaxation hardly occurs and Young's modulus of the polyimide film is obtained to be $E_f=1.18$ GPa. The residual stresses relax by an amount of 10% at 100°C and 20% at 150°C for two hours after manufacturing.

Acknowledgment

The authors would like to acknowledge many fruitful discussions with Prof. Y. Y. Earmme at KAIST. And this work has been supported by Computer Aided Reliability Evaluation (CARE) for Electronic Packaging: National Research Laboratory (NRL) program.

References

- Christensen, R. M., 1982, "Theory of Viscoelasticity," Academic Press.
- Courjon, D. et al., 1995, "New Optical Near Field Developments: Some Perspectives in Interferometry," *Ultramicroscopy*, Vol. 61, pp. 117~125.
- Findley, W. N. et al., 1976, "Creep and Relaxation of Nonlinear Viscoelastic Materials with an Introduction to Linear Viscoelasticity," North Holland Publishing Company.
- Flinn, P. A. et al., 1987, "Measurement and Interpretation of Stress in Aluminum-Based Metallization as a Function of Thermal History," *IEEE Trans. on Electronic Devices*, Vol. ED-34, No. 3, pp. 689~699.
- Hecht, E., 1998, *Optics*, Addison-Wesley.
- Hwang, H. Y. et al., 2003, "Thermo-Viscoelastic Residual Stress Analysis of Metal Liner-Inserted Composite Cylinder," *KSME International Journal*, Vol. 17, pp. 171~180.
- Kampfe, B., 2000, "Investigation of Residual Stresses in Microsystems Using X-ray Diffraction," *Material Science and Engineering*, Vol. A288, pp. 119~125.
- Laserna, J. J., 1996, "Modern Techniques in Raman Spectroscopy," John Wiley & Sons.
- Lim, J. H. et al., 2000, "A Thermomechanical Analysis of MCM-D Substrate of Polymer and Metal Multilayer," *Key Engineering Materials*, Vol. 183-187, pp. 1123~1128.
- Nix, W. D., 1989, "Mechanical Properties of Thin Films," *Metal. Trans. A*, Vol. 20A, pp. 2217~2245.
- Stoney, G. G., 1909, "The Tension of Metallic Films Deposited by Electrolysis," *Proc. Royal Soc.*, Vol. A82, pp. 172~175.
- Suwito, W. et al., 1999, "Elastic Moduli, Strength, and Fracture Initiation at Sharp Notches in Etched Single Crystal Silicon Microstructures," *J. Appl. Phys.*, Vol. 85, pp. 3519~3534.
- Timoshenko, S., 1925, "Analysis of Bimaterial Thermostats," *J. Opt. Soc. Am.*, Vol. 11, pp. 233~256.
- Ward, I. M. et al., 1993, "An Introduction to the Mechanical Properties of Solid Polymers," John Wiley & Sons.
- Witvrouw, A. et al., 1993, "Determination of the Plane Stress Elastic Constants of Thin Films from Substrate Curvature Measurements: Applications to Amorphous Metals," *J. Appl. Phys.*, Vol. 73, pp. 7344~7350.